Particle-in-Cell/Monte Carlo Collisions Model for the Reactive Sputter Deposition of Nitride Layers

Evi Bultinck,* Stijn Mahieu, Diederik Depla, Annemie Bogaerts

A 2d3v Particle-in-cell/Monte Carlo collisions (PIC/MCC) model was constructed for an Ar/N_2 reactive gas mixture in a magnetron discharge. A titanium target was used, in order to study the sputter deposition of a TiN_x thin film. Cathode currents and voltages were calculated self-consistently and compared with experiments. Also, ion fluxes to the cathode were calculated, which cause sputtering of the target. The sputtered atom fluxes from the target, and to the substrate were calculated, in order to visualize the deposition of the TiN_x film.

Introduction

Thin titanium nitride films (TiN_x) are very often fabricated by reactive magnetron sputter deposition.[1] To understand and improve the applications of (reactive) magnetron sputtering, numerical simulations are a powerful tool. Different kinds of models can be applied to simulate gas discharges, such as continuum and particle models. Because of the low pressure of magnetron discharges, a continuum model does not describe the plasma very accurately. Also, the complexity of the magnetic field makes a continuum model very inefficient.[2] To overcome these obstacles, a so-called Particle-in-cell/Monte Carlo collisions (PIC/MCC) model is more suitable.

There exist certain simple models to describe reactive sputter deposition, such as in ref.[3–5] In ref.,[6] an MCC model was proposed for this purpose, implying however that the electric fields are not calculated self-consistently. In ref.,[7] a PIC/MCC model was constructed for reactive sputtering. However, this Ar/O_2 model does not include the sputtered atoms, it does not account for target poisoning, and it does not take into account the external circuit. Since a poisoned target strongly influences the discharge characteristics,[8] poisoning plays a very important role when adding a reactive gas to the magnetron reactor. Also, the external circuit occurs to be inevitable in a PIC/MCC code for an accurate and correct description of magnetron discharges, and in general, of all DC glow discharges.[9]

As illustrated, not much research has been carried out in the area of accurate numerical modeling to describe the behavior of reactive sputter deposition of nitride layers. Therefore, there is a need for a PIC/MCC model, which describes the sputter deposition process of the metal nitride layer in a Ar/N_2 gas mixture, and which takes into account the sputtered atoms, the poisoning of the target, and the external circuit.

Description of the Magnetron Under Study

The magnetron under study in the 2d3v PIC/MCC model is a planar circular magnetron, as presented in ref.[9] An external circuit, consisting of a resistor and a voltage source, is coupled to the cathode of the discharge in order to generate a direct current (DC). The other walls are grounded. The magnetron, containing a titanium target, operates in a mixture of nitrogen and argon in different proportions, and at 300 K.

E. Bultinck, A. Bogaerts
Research group PLASMANT, Department of Chemistry, University of Antwerp, Universiteitsplein 1, 2610 Antwerp, Belgium
E-mail: evi.bultinck@ua.ac.be
S. Mahieu, D. Depla
Department of Solid State Sciences, Ghent University, Krijgslaan 281 (S1), 9000 Ghent, Belgium

Plasma Process. Polym. **2009**, *6*, S784–S788

DOI: 10.1002/ppap.200931904

Description of the Model

Particle-in-Cell/Monte Carlo Collisions (PIC) Model

The outlines of the PIC/MCC method are given in ref.[2,9–13] The particle movement is simulated with the Particle-in-cell method, which uses superparticles (SPs) to calculate self-consistently all the plasma characteristics on a grid. The collisions of the SPs are simulated with the Monte Carlo collisions module, based on collision probability functions. The extensive list of the considered collisions and their corresponding cross sections are given in a separate publication,[14] due to the limited space in this edition. The considered species are electrons, Ar^+ ions, fast Ar atoms, metastable Ar atoms, Ti^+ ions, fast Ti atoms, N_2^+ ions, N^+ ions, and fast N atoms. Moreover, thermalized Ti and N atoms are described separately with balance equations. Plasma-wall interactions are also treated (see below).

Plasma-Wall Interactions

Since magnetrons are widely used for sputter deposition purposes, the sputtering of the target is included in the model. When a particle with sufficient energy hits the cathode surface (target), a target particle can be sputtered. Each time a particle hits the cathode surface, the sputter yield is calculated and compared to a random number to define whether sputtering occurs. The sputter yield for incident particles of energy E_i is described by the empirical relation of Matsunami[15]:

$$Y(E_i) = 0.42 \frac{\alpha Q K s_n(E_i)}{U_s(1 + 0.35 U_s s_e(E_i))} \left[1 - (E_{th}/E_i)^{1/2}\right]^{2.8}, \quad (1)$$

where U_s is the sublimation energy of the cathode, E_{th} the threshold energy, and the other parameters are properties of the cathode material, as explained in ref.[15]

Electrons that hit the cathode surface can be reflected or adsorbed, characterized by the reflection coefficient (RC). Note that in magnetrons, only interaction of electrons with the cathode wall is important, so it is ignored at the other walls.

The ion- or atom-induced secondary electron emission is characterized by the secondary electron emission coefficient (SEEC) describing the amount of secondary electrons produced by an ion or atom hitting the cathode surface. Note that secondary electron emission at the other walls is again less important, so it is not included. Unfortunately, very diverse SEEC values are reported for Ti ranging from 0.075[16] to 0.148.[17] Moreover, these values describe the effective secondary electron yield, which is composed from both SEEC and RC.[18] Therefore, the exact SEEC is not known. Since both the RC and the SEEC directly influence the cathode current and voltage,[8] they are slightly adapted in the model, so that the calculated currents and voltages can be compared with experimental values. However, these coefficients were kept the same for the different current–voltage combinations investigated (see below).

Because the aim of this study is also to investigate the deposition of the TiN_x film, the interaction of Ti and N atoms with the walls is also accounted for. When a Ti or N atom collides with a wall, it can be reflected or adsorbed, depending on its sticking coefficient (SC). The SC of a reactive N atom is mostly assumed to be 1,[4] whereas the SC of Ti is found to be dependent on target-substrate distance.[19] In accordance to these reported values,[19] a SC_{Ti} of 0.5 is chosen in our model. The SC of the background gases are assumed in the model to be 0. For Ar being an inert gas, a zero sticking approximation is justified. The partial pressure of N_2 is used in the code as measured experimentally. In the model, this constant partial pressure corresponds to the assumption of zero effective sticking for N_2. Moreover, the SC of N_2 is very low, and its influence on the calculated N_2 density is therefore negligible, which also justifies the assumption.

Effect of Poisoning on the Plasma-Wall Interactions

When a reactive gas, for example nitrogen, is added to the argon background gas, it can react with the cathode atoms to form a TiN_x layer.[20] This process is called "poisoning", and influences the plasma-wall interactions, and therefore all of the calculated plasma characteristics. The transition from the so-called metallic to poisoned mode happens via a hysteresis.[20,21] In the present work, we used N_2 gas flows for which the target is already in poisoned mode, in order to avoid (i) the simulation of the hysteresis, and (ii) having to deal with a partially N-covered Ti target, which would include for example the need for using a radially dependent SEEC value and sputter yield.

When the target is poisoned, both Ti and N atoms can be sputtered, however, with a lower sputter yield. The sputter yield of Ti and N is therefore adjusted in accordance to reported values.[4]

Moreover, poisoning of the target causes the cathode potential to change. This is a consequence of a change of the SEEC.[18] In the model, the poisoning of the target is therefore described by changing the SEEC value. As for the case of a metallic target, the SEEC of a poisoned target is not exactly known. Therefore, it is also slightly tuned, of course within a reasonable range,[18] so that the calculated current and voltage values are in reasonable agreement with experiment.

Table 1. Measured and calculated values of the cathode potentials (V) and currents (I) for a pure argon gas flow of 60 sccm (1.0 Pa), an external voltage of −600 V, and external resistances (R_{ext}) as mentioned in the table.

Measured		Calculated		Input
V	*I*	*V*	*I*	R_{ext}
V	A	V	A	Ω
−260	0.20	−255	0.23	1500
−264	0.23	−257	0.25	1400
−266	0.26	−257	0.26	1300

Results and Discussion

Pure Ar Gas: Current–Voltage (*I–V*) Characteristics

The following input values were used for the Ar pressure, external voltage, RC, SEEC, and SC_{Ti}: 1.0 Pa (60 sccm), −600 V, 0.1, 0.075,[16] and 0.5,[19] respectively. The discharge current and potential were varied by modifying the external resistance, as 1 500, 1 400, and 1 300 Ω. The calculations are carried out until convergence is reached, typically around a simulated time of 15 μs. The calculated and experimental values of the current and the potential are presented in Table 1.

Reactive Ar/N_2 Gas Mixture: the Effect of Poisoning

The input values for the Ar pressure, the external voltage, RC, $SC_{Ti,}$ and SC_N are 1.0 Pa (60 sccm), −600 V, 0.1, 0.5,[19] and 1,[4] respectively. The cathode current was kept constant at 0.2 A, by keeping the external resistance at 1500 Ω. Calculations were carried out for different nitrogen partial pressures (0.03, 0.06, 0.13, 0.19, and 0.26 Pa, which correspond to gas flows of 2.5, 5, 10, 15, and 20 sccm, respectively). Under these conditions, the target is always fully poisoned, so that the hysteresis behavior can be avoided.

Table 2. SEEC values at the different nitrogen gas flows, used in the model to simulate poisoning of the target.

N_2	SEEC
sccm	
0	0.075
2.5	0.070
5	0.065
10	0.060
15	0.055
20	0.050

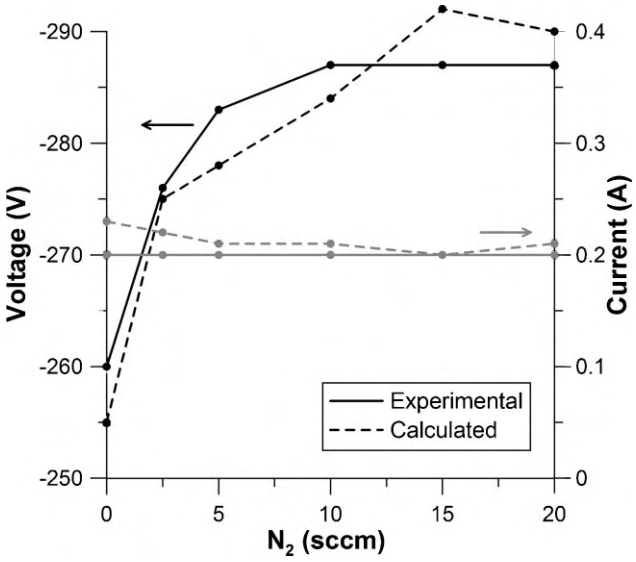

Figure 1. Measured and calculated values of the cathode potentials and currents as a function of nitrogen gas flow, for an argon gas flow of 60 sccm (1.0 Pa), an external voltage of −600 V, and an external resistance (R_{ext}) of 1 500 Ω.

The sputter yields of Ti and N, sputtered from a poisoned target (denoted as Y_{Ti} (TiN_x) and Y_N (TiN_x), respectively) are evaluated toward the sputter yield of Ti from a metallic target (Y_{Ti} (Ti)), according to the values calculated in ref.[4] This means that the sputter yield of Ti from a TiN_x target is lowered with a factor of 6.4 compared to the sputter yield of Ti from a Ti target (Y_{Ti} (TiN_x) = Y_{Ti} (Ti)/6.4), and the sputter

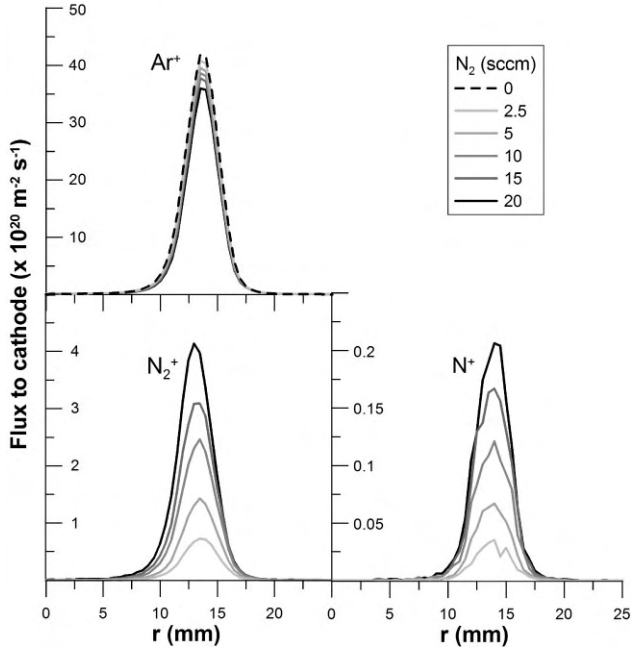

Figure 2. Calculated ion fluxes to the cathode for different nitrogen gas flows, and for an argon gas flow of 60 sccm (1.0 Pa).

DOI: 10.1002/ppap.200931904

yield of N from a TiN_x target is analogously lowered with a factor of 1.6 ($Y_N(TiN_x) = Y_{Ti}$ (Ti)/1.6). Radially dependent sputter yields do not have to be taken into account, since the target is fully in poisoned mode at the used N_2 pressures.

As mentioned before, also the SEEC will change due to poisoning. In the case of a TiN_x target, the SEEC decreases.[18] The values used for different N_2 gas flows are presented in Table 2. It is worth mentioning that these SEEC values comprise the SEEC values of all different incident species, i.e., no distinction is made between the SEEC of an Ar^+ ion and a $N(_2)^+$ ion. These two approximations are done to avoid complicating the model with different uncertain parameters. Furthermore, as mentioned before, the target is completely in poisoned mode, so the SEEC value will barely alter radially on the surface. Therefore, the use of a constant radial SEEC value in the model is justified.

From Table 2, it is clear that this overall SEEC decreases with increasing N_2 flow. However, in reality, the SEEC value of individual species will probably decrease first, but then remain constant. Nevertheless, the proportion $N(_2)^+/Ar^+$ will increase with N_2 flow, and because the SEEC of $N(_2)^+$ is much lower[22] than the SEEC of Ar^+ the overall SEEC will indeed decrease with increasing N_2 flow.

The calculated currents and voltages as a function of N_2 gas flow are illustrated in Figure 1, as well as the experimental values.

The calculated ion fluxes to the cathode for different N_2 gas flows are presented in Figure 2. They all exhibit a maximum at 13.5 mm from the central axis, i.e., where the radial magnetic field is at maximum. This causes the electrons to be trapped there, leading to an enhanced ionization in this region. When the N_2 flow is increased, the N_2^+ and N^+ fluxes increase, whereas the Ar^+ flux decreases. However, the total ion flux to the cathode is approximately constant.

These ion fluxes to the cathode cause sputtering of the target, as shown in Figure 3. Again, a maximum is apparent at 13.5 mm, which corresponds to the race-track of the target. Figure 3a shows that the sputtered Ti flux of a poisoned target is approximately a factor of 8 lower than for a metallic target due to the lower sputter yield. Once the target is poisoned, the sputtered Ti flux remains constant, as a consequence of the constant ion flux to the cathode (see above). The sputtered N flux, presented in Figure 3b, is higher than the sputtered Ti flux due to the higher sputter yield of N. In contrast to the Ti flux, the N flux increases slightly with increasing N_2 gas flow. This is explained as follows: the sputter yield of N is higher with N_2^+ or N^+ than with Ar^+ bombardment, whereas the sputter yield of Ti is less dependent of the incoming ion. With increasing the N_2 flow, the N_2^+ and N^+ fluxes increase (see Figure 2), hence leading to a slightly enhanced sputtering of N.

The sputtered atoms diffuse through the plasma and can be deposited on the substrate, located at the anode opposite to the target. The calculated fluxes of Ti and N atoms to the substrate are presented in Figure 4. The Ti flux to the substrate (Figure 4a) has a similar peak profile as the sputtered Ti flux, however, it is broadened by diffusion through the plasma. Similar to the sputtered Ti flux, the Ti

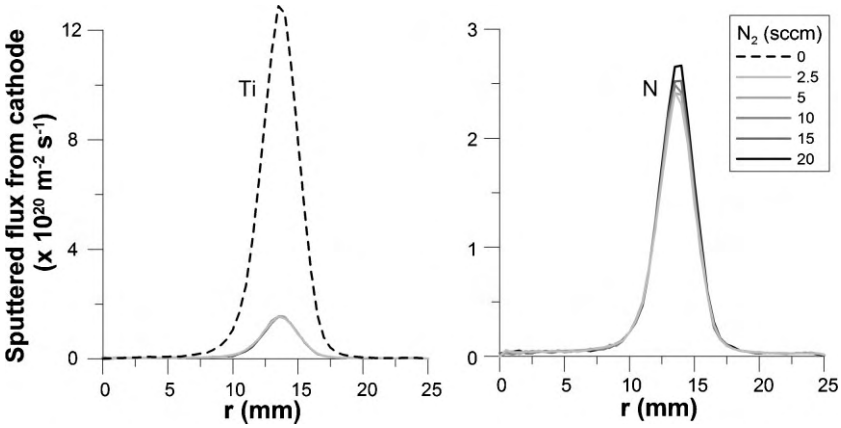

Figure 3. Calculated sputtered Ti and N fluxes from the cathode for different nitrogen gas flows, and for an argon gas flow of 60 sccm (1.0 Pa).

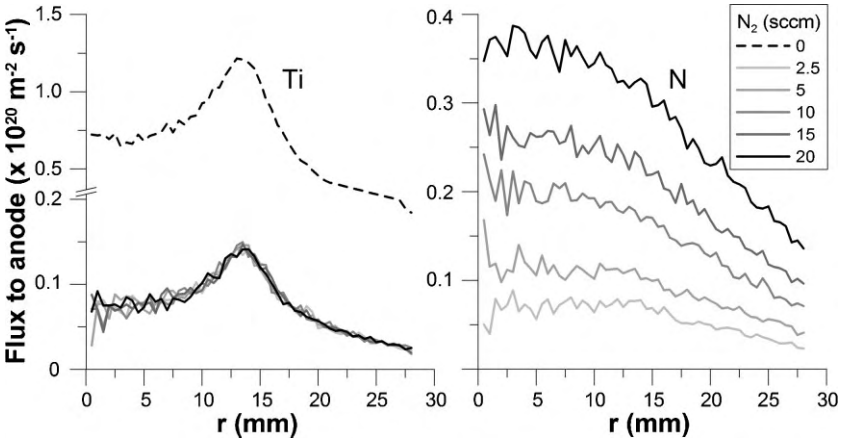

Figure 4. Calculated Ti and N fluxes to the anode for different nitrogen gas flows, and for an argon gas flow of 60 sccm (1.0 Pa).

flux to the anode shows a pronounced drop when adding N_2 gas, and stays constant with further increasing the N_2 flow. From Figure 4b, it is clear that the N flux to the substrate has lost the peak profile, which was seen in the sputter profile (Figure 3b). This is explained by the fact that N atoms are also created by the N_2 gas in the plasma, and do not only originate from sputtering of the TiN_x target. These N atoms cause a typical diffusion profile. When a lot of N is created in the plasma, the peak from the sputtering will disappear in the diffusion profile. The more N_2 gas is added, the more N is created in the plasma, and the larger the N flux to the substrate, as is clear from Figure 4b.

Conclusion

A PIC/MCC model was developed which is able to simulate the reactive sputter deposition process in a magnetron discharge. This accurate modeling approach was validated by comparing calculated and experimental currents and voltages. Ion fluxes to the target were calculated, which explain the sputter process, characterized by the fluxes of sputtered Ti and N atoms from the target. The fluxes of Ti and N atoms to the substrate were calculated to try to comprehend the deposition of the TiN_x thin film. With this model, we are able to visualize very accurately the physical processes that occur in a magnetron discharge, leading to a better understanding of the reactive sputter deposition of thin films.

Acknowledgements: *E. Bultinck* is indebted to the *University of Antwerp* for financial support. *S. Mahieu* is indebted to the FWO-Flanders for his postdoctoral fellowship. The computer facility CALCUA from the *University of Antwerp* is acknowledged.

Received: September 29, 2008; Accepted: March 15, 2009; DOI: 10.1002/ppap.200931904

Keywords: magnetron; modeling; plasma; sputter deposition

[1] S. Mahieu, P. Ghekiere, G. De Winter, R. De Gryse, D. Depla, G. Van Tendeloo, O. I. Lebedev, *Surf. Coat. Technol.* **2006**, *200*, 2764.
[2] I. Kolev, A. Bogaerts, *Contrib. Plasma Phys.* **2004**, *44*, 582.
[3] S. Berg, T. Nyberg, *Thin Solid Films* **2005**, *476*, 215.
[4] W. Möller, D. Güttler, *J. Appl. Phys.* **2007**, *102*, 094501.
[5] D. Depla, S. Heirwegh, S. Mahieu, R. De Gryse, *J. Phys. D: Appl. Phys.* **2007**, *40*, 1957.
[6] A. Pflug, B. Szyszka, J. Niemann, *Thin Solid Films* **2003**, *442*, 21.
[7] K. Nanbu, K. Mitsui, S. Kondo, *J. Phys. D: Appl. Phys.* **2000**, *33*, 2274.
[8] D. Depla, S. Heirwegh, S. Mahieu, J. Haemers, R. De Gryse, *J. Appl. Phys.* **2007**, *101*, 013301.
[9] E. Bultinck, I. Kolev, A. Bogaerts, D. Depla, *J. Appl. Phys* **2007**, *103*, 013309.
[10] C. K. Birdsall, A. B. Langdon, *Plasma Physics via Computer Simulations*, IOP publishing, Bristol 1991.
[11] I. Kolev, A. Bogaerts, R. Gijbels, *Phys. Rev. E* **2005**, *72*, 056402.
[12] I. Kolev, A. Bogaerts, *IEEE Trans.Plasma Sci.* **2006**, *34*, 886.
[13] I. Kolev, A. Bogaerts, *Plasma Process. Polym.* **2006**, *3*, 127.
[14] E. Bultinck, S. Mahieu, D. Depla, A. Bogaerts, *New J. Phys.* **2009**, *11*, 023039.
[15] N. Matsunami, Y. Yamamura, Y. Itikawa, N. Itoh, Y. Kazumata, S. Miyagawa, K. Morita, R. Shimizu, H. Tawara, *Atom. Data Nucl. Data* **1984**, *31*, 1.
[16] M. A. Lewis, D. A. Glocker, J. Jorne, *J. Vac. Sci. Technol., A* **1989**, *7*, 1019.
[17] H. Oechsner, *Phys. Rev. B* **1978**, *17*, 1052.
[18] D. Depla, X. Y. Li, S. Mahieu, R. De Gryse, *J. Phys. D: Appl. Phys.* **2008**, *41*, 202003.
[19] S. Mahieu, K. Van Aeken, D. Depla, D. Smeets, A. Vantomme, *J. Phys. D: Appl. Phys.* **2008**, *41*, 152005.
[20] D. Depla, R. De Gryse, *Plasma Sources Sci. Technol.* **2001**, *10*, 547.
[21] D. Depla, H. Tomaszewski, G. Buyle, R. De Gryse, *Surf. Coat. Technol.* **2006**, *201*, 848.
[22] R. A. Baragiola, E. V. Alonso, J. Ferron, A. Olivaflorio, *Surf. Sci.* **1979**, *90*, 240.